J3.5 NUMERICAL SIMULATIONS OF URBAN HEAT ISLANDS AND TRANSPORT AND DISPERSION OF AIRBORNE MATERIALS AROUND BUILDING CLUSTERS

Tetsuji Yamada*
Yamada Science & Art Corporation, Santa Fe, New Mexico

1. INTRODUCTION

Urbanization has drastically increased at an alarming rate. In the 1800's, only three percent of the world's population lived in urban areas. By the 1950's, thirty percent were urbanized and in 2000 about forty seven percent lived in urban areas (UN, 1999). The number of mega-cities (population of 10 million or more people) dramatically increased from four in 1975 to eighteen in 2000. The United Nations estimates there will be around twenty-two mega-cities by 2015 (UN, 2003).

With this ever-increasing growth came numerous problems such as air pollution associated with emissions from automobiles and plants, and temperature increases associated with human activities to name a few. Both issues are considered to be the major contributors to the global warming.

Urban areas are known to be warmer than the surrounding rural areas (so called "urban heat island"). Bare soils and vegetated surfaces are replaced by concrete structures and pavements which absorb and store more heat from the sun than the original surfaces. The heat energy stored in the pavements and concrete structures heat air during the night time. Urban heat island effect is further enhanced by exhaust heat associated with human activities such as air conditioning and manufacturing.

The urban heat island coupled with adverse weather conditions creates serious health problems. Heat waves are blocked by high rises and stay in urban areas causing heat strokes and discomforts to the people living in the urban areas.

Recently, there have been some efforts in combining the CFD (Computational Fluid Dynamics) and atmospheric models capabilities to address effects on air flows from building scales to terrain scales. This is what is required to simulate air flows over the urban areas in complex terrain and/or coastal areas. This paper effects on air flows from a building to terrain scales. This is what is required discusses how an atmospheric model HOTMAC was improved to simulate air flows around buildings under the influence of mesoscale wind variations.

2. MODELS

To address building scales we have added CFD capabilities to a three-dimensional mesoscale model HOTMAC. The new model is referred to as A2Cflow where "A2C" stands for "Atmosphere to CFD." The model capabilities of A2Cflow have been greatly enhanced from those for HOTMAC.

The governing equations for mean wind, temperature, mixing ratio of water vapor, and turbulence are similar to those used by Yamada and Bunker (1988). Turbulence equations were based on the Level 2.5 Mellor-Yamada second-moment turbulence-closure model (1974, 1982). Five primitive equations were solved for ensemble averaged variables: three wind components, potential temperature, and mixing ratio of water vapor. In addition, two primitive equations were solved for turbulence: one for turbulence kinetic energy and the other for a turbulence length scale (Yamada, 1983).

The hydrostatic equilibrium is a good approximation in the atmosphere. On the other hand, air flows around buildings are not in the hydrostatic equilibrium. Pressure variations are generated by changes in wind speeds, and the resulted pressure gradients subsequently affect wind distributions. We adopted the HSMAC (Highly Simplified Marker and Cell) method (Hirt and Cox, 1972) for non-hydrostatic pressure computation because the method is simple yet efficient. The method is equivalent to solving a Poisson equation, which is commonly used in non-hydrostatic atmospheric models.

* *Corresponding author address*: Tetsuji Yamada, Yamada Science & Art Corporation, 13 Heiwa, Santa Fe, NM 87506; e-mail: ysausa@ysasoft.com

Boundary conditions for the ensemble and turbulence variables are discussed in detail in Yamada and Bunker (1988). The temperature in the soil layer is obtained by numerically integrating a heat conduction equation. Appropriate boundary conditions for the soil temperature equation are the heat energy balance at the ground and specification of the soil temperature at a certain distance below the surface, where temperature is constant during the integration period. The surface heat energy balance is composed of solar radiation, long-wave radiation, sensitive heat, latent heat, and soil heat fluxes.

Lateral boundary values for all predicted variables are obtained by integrating the corresponding governing equations, except that variations in the horizontal directions are all neglected. The upper level boundary values are specified and these values are incorporated into the governing equations through a four-dimensional data assimilation or a "nudging" method (Kao and Yamada, 1988).

Temperatures of building walls and roofs were computed by solving a one-dimensional heat conduction equation in the direction perpendicular to the walls and roofs. The boundary conditions were a heat balance equation at the outer sides of walls and roofs and room temperatures specified at the inner sides of the walls.

3. SIMULATIONS

We conducted three case studies to demonstrate the thermal effects of buildings on the air flows and transport and diffusion of airborne materials around buildings.

The first case assumed the building wall temperatures were the same as the air temperature adjacent to the walls. The second case represented the afternoon (2 p.m.) condition when the walls facing west were heated by the sun. The third case represented the night time (3 a.m.) condition when wall temperatures were less than the air temperatures adjacent to the walls. Building wall temperatures decreased by long wave radiation cooling.

The computational domain was 200 m x 200 m in the horizontal direction and 500 m in the vertical direction. Horizontal grid spacing was 4 m and the vertical grid spacing was 4 m for the first 15 levels and increased spacing gradually with height. There were 31 levels in the vertical direction.

Two buildings were placed along the center axis of the computational domain. The size of each building was 32 m x 32 m in the base and 30 m in height. Initial winds were westerly and 5 m/s throughout the computational domain Boundary conditions for winds were 5 m/s at the inflow boundary and in the layers higher than 200 m from the ground. The boundary conditions were maintained through a nudging method.

The initial potential temperature was 25 C at the ground and increased with height with a lapse rate of 1 C/1000 m up to the height 200 m above the ground. The lapse rate increased to 3 C/1000 m in the layer higher than 200 m from the ground. The initial potential temperatures were uniformly distributed in the horizontal direction.

Fig. 1 shows the modeled wind distributions for Case 1 in a vertical cross section along the centerline of the computational domain. The wall temperatures were assumed to be the same as the air temperatures.

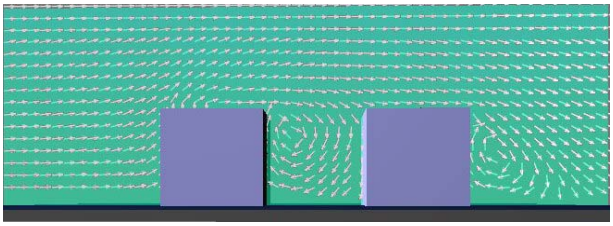

Fig. 1: The modeled wind distributions in a vertical cross section along the centerline of the computational domain. Case 1: wall temperatures were assumed to be the same as the air temperatures adjacent to the walls.

There were upward motions at the leading edge of the first building (left hand side), which resulted in separation and recirculation of air flows along the roof. Separation of air flows also occurred at the rear side of each building. The modeled characteristics of recirculation and reattachment were in good qualitative agreement with wind tunnel data.

Diurnal variations of building wall temperatures were obtained by solving a one-dimensional heat conduction equation in the direction perpendicular to the wall surfaces. The boundary conditions were the heat energy balance at the outer surfaces and constant temperature (25 C) specified at the inner surfaces.

Fig. 2 shows the modeled wind distributions at 2 p.m. in a vertical cross section along the centerline of the computational domain. The temperature on the wall facing west was approximately 40 C, which was significantly higher than the temperature on the wall facing east (approximately 20 C).

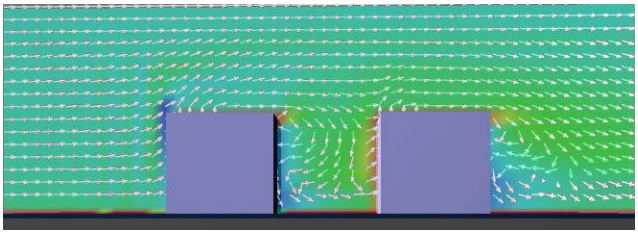

Fig. 2: The modeled wind distributions in a vertical cross section along the centerline of the computational domain at 2 p.m. (Case 2). Arrows indicate wind direction and colors indicate temperatures: red for 40 C and green for 25 C.

Recirculation flows between the two buildings no longer existed. There were upward motions along the warmer walls and downward motions along the cooler walls.

Fig. 3 shows the modeled wind distributions at 2 a.m. in a vertical cross section along the centerline of the computational domain.

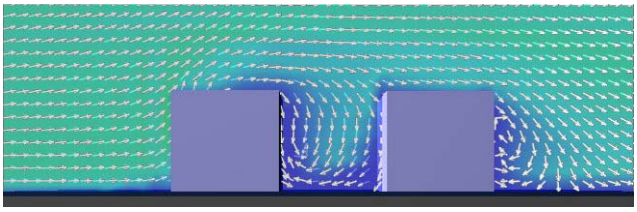

Fig. 3: The modeled wind distributions in a vertical cross section along the centerline of the computational domain at 2 a.m. (Case 3). Arrows indicate wind directions and colors indicate temperatures: blue for 20 C and green for 25 C.

Temperatures at building walls decreased due to long wave radiation cooling and became lower than the air temperatures adjacent to the walls.

Consequently, downward motions occurred along the vertical walls between the two buildings. The air flows reached the ground and diverged sideway.

It is obvious from the above discussions that air flows around buildings were quite different whether building wall temperatures were higher or lower than the air temperatures. Thermal effects of building walls on air flows were qualitatively verified by observations of soap bubbles released near warm or cold building walls.

To illustrate three-dimensional air flows, particles were released at the ground between the two buildings. Animations will be shown at the presentation.

We simulated diurnal variations of air flows around a cluster of buildings, which were bound by the ocean and hills. Large cities are often located in a coastal area or near complex terrain. Prediction of transport and diffusion of air pollutants and toxic materials is a considerable interest to the safety of the people living in urban areas.

Two inner domains were nested in a large domain (Fig. 4). The first domain was 6560 m x 8960 m with horizontal grid spacing of 160 m. The second domain was 1280 m x 1440 m with horizontal grid spacing of 40 m. The third domain was 360 m x 400 m with horizontal grid spacing of 10 m.

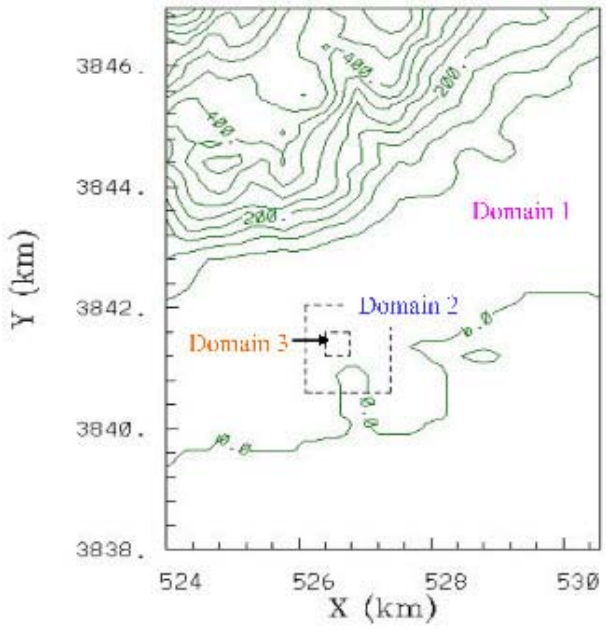

Figure 4: Computational domains: Domain 1 is the outer domain. Solid contour lines indicate ground elevations. Numerical numbers are altitudes in meters. Dashed lines indicate boundaries of nested domains: Domain 2 and Domain 3.

Domain 1 includes topographic features such as the ocean, coastal area, plains, and hills. Domain

2 is a transition area between Domain 1 and Domain 3. Buildings were located in Domain 3.

There were significant differences in wind distributions around building clusters whether building walls were heated or not. Fig.5 shows wind and temperature distributions at 9 a.m. in a vertical cross section of east and west direction.

Arrows indicate wind directions and colors indicate temperatures. Temperatures along the walls facing east were significantly higher than those along the walls facing in other directions.

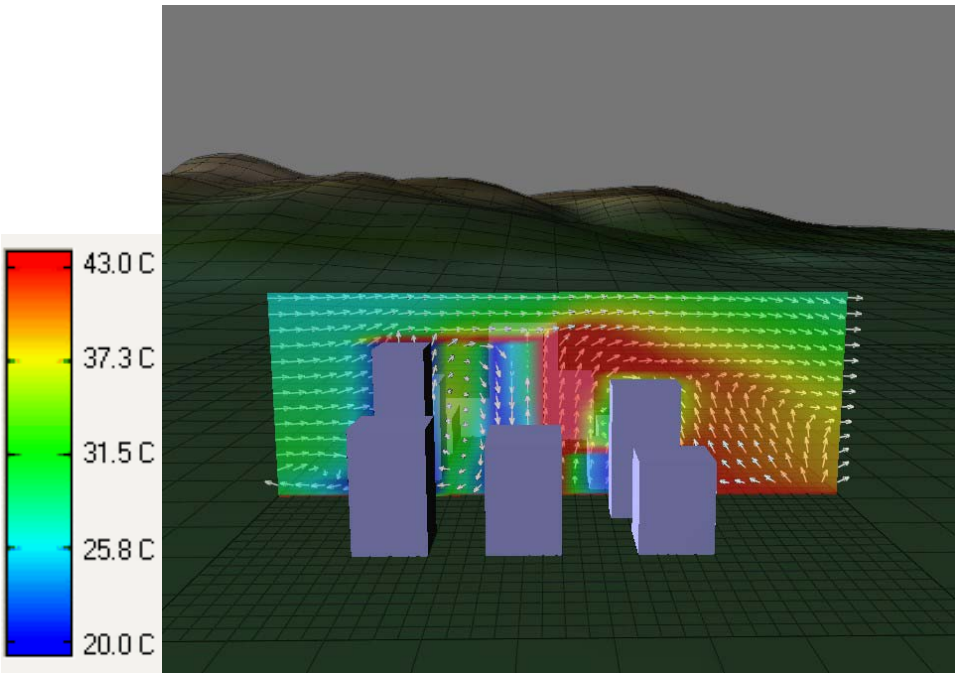

4. SUMMARY

A three-dimensional atmospheric prediction model, HOTMAC, was improved so that airflows not only in complex terrain, but also around buildings and wind tunnel data were simulated. We adopted HSMAC method for the non-hydrostatic pressure computation because it is simple yet efficient. The method is equivalent to solving a Poisson equation, which is commonly used in non-hydrostatic atmospheric models.

Building wall temperatures were computed by solving a one-dimensional heat conduction equation in a direction perpendicular to walls. Boundary conditions were a heat energy balance at the outer surfaces of buildings and temperatures specified at the inner surfaces.

Three case simulations were conducted to illustrate the thermal effects of building walls on the air flows around two (2) buildings. For Case 1 wall temperatures were assumed to be the same as the air temperatures adjacent to building walls.

Case 1 was a control run where wind distributions were similar to those observed in a wind tunnel. Separation and reattachment of air flows at the leading edge and behind buildings were in good agreement of wind tunnel data.

When building walls were heated and cooled, air flows around two buildings became quite different from those in Case 1. Recirculation and reattachment around buildings no longer existed.

In general upward motions were simulated along warm walls and downward motions were simulated along cold walls.

We simulated diurnal variations of air flows around a cluster of buildings, which were bound by the ocean and hills. Large cities are often located in a coastal area or near complex terrain. Prediction of transport and diffusion of air

pollutants and toxic materials is of considerable interest to the safety of the people living in urban areas.

We deployed nested grids: Domain 1 was 6560 m x 8960 m with horizontal grid spacing of 160 m. Domain2 was 1280 m x 1440 m with 40 m grid spacing and nested in Domain 1. Domain 3 was 360 m x 400 m with10 m grid spacing and nested in Domain 2.

There were significant interactions between air flows generated by topographic variations and a cluster of buildings. Sea breeze fronts were retarded by buildings. Winds were calm in the courtyards. Winds diverged in the upstream side and converged in the downstream side of the building cluster.

Wind speeds and wind directions around buildings changed as the winds in the outer domains encountered diurnal variations. Domain 3 alone could not reproduce diurnal variations of winds because it didn't include topographic features responsible for mesoscale circulations such as sea/land breezes and mountain/valley flows.

On the other hand, Domain 1 alone could not depict the effects of buildings because the horizontal grid spacing (160 m) was too coarse to resolve buildings. Air flows around buildings were successfully simulated in Domain 3 and modified air flows in Domain 3 were transferred back to Domain 2 and Domain 1 through two-way nesting algorithm.

A few atmospheric models have both mesoscale and CFD scale modeling capabilities. However, we are not aware of any report that a single model was used to simulate interactions between mesoscale and CFD scale circulations.

REFERENCES

Hirt, C.W., and J. L. Cox, 1972: Calculating Three-Dimensional Flows around Structures and over Rough Terrain. *J. of Computational Phys*., **10**, 324-340.

Kao, C.-Y. J. and Yamada, T., 1988: Use of the CAPTEX Data for Evaluation of a Long-Range Transport Numerical Model with a Four-Dimensional Data Assimilation Technique, *Monthly Weather Review*, **116**, pp. 293-206.

Mellor, G. L., and T. Yamada, 1974: A Hierarchy of Turbulence Closure Models for Planetary Boundary Layers. *J. of Atmos. Sci*., **31**, 1791-1806.

Mellor, G. L., and T. Yamada, 1982: Development of a Turbulence Closure Model for Geophysical Fluid Problems. *Rev. Geophys. Space Phys*., **20**, 851-875.

United Nations, World Urbanization Prospects, The 1999 revision.

United Nations, World Urbanization Prospects, The 2003 revision.

Yamada, T., 1983: Simulations of Nocturnal Drainage Flows by a q^2l Turbulence Closure Model. *J. of Atmos. Sci*., **40**, 91-106.

Yamada, T., and S. Bunker, 1988: Development of a Nested Grid, Second Moment Turbulence Closure Model and Application to the 1982 ASCOT Brush Creek Data Simulation. *Journal of Applied Meteorology*, **27**, 562-578.